

© 2020. A. Urbański, M. Richter.

This is an open-access article distributed under the terms of the Creative Commons Attribution-NonCommercial-NoDerivatives License (CC BY-NC-ND 4.0, <https://creativecommons.org/licenses/by-nc-nd/4.0/>), which permits use, distribution, and reproduction in any medium, provided that the Article is properly cited, the use is non-commercial, and no modifications or adaptations are made.



# STABILITY ANALYSIS OF DRILLING RIGS MOVING ON A WEAK SUBSOIL. SELECTED CASE STUDIES

A. URBAŃSKI<sup>1</sup>, M. RICHTER<sup>2</sup>

This article presents results of the numerical analysis of the interaction between heavy caterpillar tracks system and subsoil. The main goal of the article is to present an algorithm to design working platforms - temporary structures enabling the work of heavy construction equipment on weak subsoils. A semi-analytical method is based on the results of the numerical analysis performed with use of the finite element method (FE software ZSoil.PC [12]). The calculations were carried out for the piling rig machine - Bauer BH20H (BT60). Three ground models were adopted: Model 1: one layer - weak cohesive soil (clay); Model 2: two layers: weak cohesive soil (clay) and cohesionless working platform (medium sand); Model 3: one layer: strong cohesionless subsoil (medium sand). The following problems were solved: I) entry of the machine on the ground with various geotechnical parameters under each caterpillar tracks II) detection of the maximum permissible angle of ground slope.

*Keywords:* Working platforms, Subsoil-machine interaction, Piling rig machine, Bearing capacity, Geotechnical engineering, Finite element modeling

<sup>1</sup>DSc., PhD., Eng., Assistant professor at Cracow University of Technology, Faculty of Civil Engineering, ul. Warszawska 24, 31-155 Cracow, Poland, e-mail: aurbansk@pk.edu.pl

<sup>2</sup>MSc., Eng., Cracow University of Technology, Faculty of Environmental and Energy Engineering, ul. Warszawska 24, 31-155 Cracow, Poland, e-mail: richter.mateusz@student.pk.edu.pl

## 1. INTRODUCTION

Heavy machines (piling rigs, drilling rigs) used on construction sites to perform foundation piles have a weight reaching up to 200 tons with all equipment and a highly located center of gravity (to increase the diameter of the piles and to increase drilling depth). The center of gravity varies depending on the working phase (transport, movement on construction site, working etc.). In the case of insufficient bearing capacity of the subsoil on which the machine needs to work, it is necessary to make a temporary structure - working platform, enabling entry of the tracked vehicle to the final destination on the construction site. Accidents involving collapse of piling rig occur several times a year. Not all accidents are reported to the public information by contractors. Therefore, working platforms should be subject to a standard design process.

The document constituting the guide for the design of working platforms was issued by the Building Research Establishment Ltd (BRE) [11] in cooperation with FPS (Federation of Piling Specialists) [8]. This guide provides information on the design, implementation and operation of work platforms built of aggregate or aggregate in cooperation with geosynthetics. The calculation method shown in the document is applicable if the shear strength without ground drainage assumes a value of 20kPa - 80kPa, therefore it does not apply to weak subsoils, whose shear strength is usually less than 20kPa.

Most of the publications examining this matter restrict themselves to the problem of the bearing capacity of layered subsoil, with assumed plane strain conditions. It concerns bearing capacity of subsoil loaded only with one caterpillar track. One of the first was the semi-empirical theory proposed by Hanna and Meyerhof [5]. Another solution came from Burd and Frydman [2], W.F. Chen and H.L. Davidson [3], Griffiths [4], Michałowski and Shi [6] and Mitchell [7]. Recently, upper bound estimates have been proposed – and then compared with the BRE [11] – by Białek et al. [1], using Distinct Layout Optimization.

Consistent mechanical approach analysing interaction of two caterpillar tracks in the moving stage of drilling rigs on weak subsoil (with or without a working platform) is the main goal proposed by Urbański et al. [10]. The assumptions contained in [10], reminded also in chapter 2, constitute the basis and introduction to the considerations contained in this article.

## 2. ASSUMPTIONS

Mechanical model of the analyzed machine-subsoil system is formulated based on the following assumptions:

- 1) The machine is moving on a caterpillar tracks system (exclusively). Machines moving on wheels are not considered in this article.
- 2) The whole machine, including its two caterpillar tracks, is treated as a perfectly rigid body.
- 3) The subsoil is treated as an elastic perfectly-plastic continuum in which Mohr-Coulomb (M-C) yield criterion is used. It is characterized by two strength parameters i.e. friction angle  $\phi$  and cohesion  $c$  for fully drained conditions; in case of impermeable soils it can be reduced to the Tresca model in which undrained shear strength  $s_u$  is used as a unique strength parameter. This is the simplest choice, recommended by majority of design standards (i.e. Eurocode EC 7) for the limit state of bearing capacity of a subsoil. Other options of constitutive modeling were also discussed, i.e. usage of HSS model which recently is widely considered as the best model in structure-soil interaction problem, and was implemented in ZSoil.PC [12] which we used to create data to our analytical model. However, as our data were related to some real geotechnical records from which there was impossible to identify parameters required by HSS. Moreover, the main our interest was in the situation close to the limit state in which HSS and Mohr-Coulomb coincide.
- 4) The overlapping zones of impacts of individual caterpillar tracks on the subsoil have been omitted.

The basic equations of equilibrium with their description are included in the article [10].

The basic formulas quoted from this article are given below:

$$(2.1) \quad Q_1 + Q_2 = Q$$

$$(2.2) \quad M_1 + M_2 = M_X$$

$$(2.3) \quad Q_1 \cdot \frac{D}{2} - Q_2 \cdot \frac{D}{2} = M_Y$$

where:

$Q_i, i=1,2$  – machine weight load on one caterpillar track [kN]

$Q$  – total machine weight [kN]

$M_i, i=1,2$  – moment acting on one caterpillar track [kNm]

$M_X, M_Y$  – overall moment in the X, Y direction [kNm]

$D$  – axial distance between two caterpillar tracks [m]

$L$  – length of one caterpillar track [m]

$B$  – width of one caterpillar track [m].

After introducing a dimensionless factor describing the distribution of the total machine weight  $Q$  between two caterpillar tracks:  $\zeta_i = \frac{Q_i}{Q}, i=1,2, 0 \leq \zeta_i \leq 1$  as well as dimensionless eccentricities in the X, Y direction:  $e_X = \frac{2M_X}{Q \cdot L}, e_Y = \frac{2M_Y}{Q \cdot D}$ , and dimensionless eccentricities of forces acting on the one caterpillar track  $i=1,2: e_i = \frac{2M_i}{Q_i \cdot L}, e_X, e_Y, e_i \in \langle 0; 1 \rangle$  we have:

$$(2.4) \quad \zeta_1 + \zeta_2 = 1$$

$$(2.5) \quad \zeta_1 \cdot e_1 + \zeta_2 \cdot e_2 = e_X$$

$$(2.6) \quad \zeta_1 \cdot e_1 - \zeta_2 \cdot e_2 = e_Y$$

Statical and kinematical models of machine-subsoil system are shown in Fig. 1.

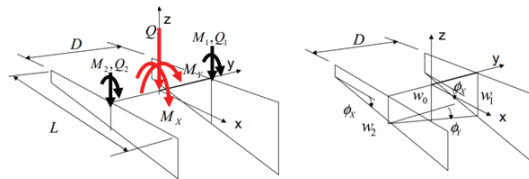


Fig. 1. Basic components of static and kinematical models.

Equation set (2.4) – (2.6) is completed by the forth equation:

$$(2.7) \quad \Phi_X(\zeta_1, Q, e_1) = \Phi_X(\zeta_2, Q, e_2),$$

coming from basic assumption of rigidity, expressing equality of rotation around Y axis of both caterpillar tracks. The machine-subsoil interaction problem is solved using FE software ZSoil.PC [12] in which subsoil and working platform are modeled as an elastic-plastic continuum, using fully drained conditions for the working platform and fully undrained conditions for the weak subsoil,

while the machine base is treated as a quasi-rigid structure. Characteristics rotation - eccentricity for different models of subsoil are shown in Fig. 2.

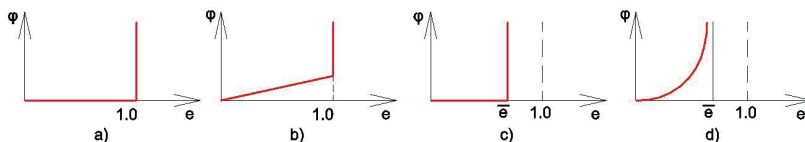


Fig. 2. Characteristics rotation - eccentricity of subsoil-rigid body system (caterpillar tracks) in unilateral contact problem for the case of subsoil type : a) rigid b) elastic c) rigid-plastic d) elastic-plastic

The limit value of the eccentricity  $\bar{e}$  appears in Fig. 2c and Fig. 2d. In this article the subsoil is treated as an elastic-plastic one (Fig. 2d).

### 3. ANALYSIS

Three subsoil cases were adopted:

- 1) MODEL 1: one layer - weak cohesive soil (clay), fully saturated:  $s_u=20\text{kPa}$ ,  $E=15\text{MPa}$ ,
- 2) MODEL 2: two layers: weak cohesive soil (clay):  $s_u=20\text{kPa}$ ,  $E=15\text{MPa}$  and cohesionless working platform (medium sand): thickness  $H=0.5\text{m}$ ,  $\phi=32^\circ$ ,  $c=5\text{kPa}$ , dilatancy angle  $\psi=8^\circ$ ,  $E=80\text{MPa}$ .
- 3) MODEL 3: one layer: strong cohesionless subsoil (medium sand) - geotechnical parameters same as working platform in Model 2

Material properties for soils used in FE models are summarized in Table 1. FE models of the machine-subsoil system are shown in Fig. 3 and Fig. 4.

Table 1. Material properties of soils

Parameter	Unit	Model 1	Model 2		Model 3
		Only Subsoil („Weak” subsoil)	Subsoil („Weak” subsoil)	Working Platform („Strong” subsoil)	Only Subsoil* („Strong” subsoil)
$E$	[kPa]	15000	15000	80000	80000
$\nu$	[-]	0.499	0.499	0.3	0.3
$\phi$	[°]	-	-	32	32
$\psi$	[°]	-	-	8	8
$s_u$	[kPa]	20	20	-	-
$\gamma$	[kN/m <sup>3</sup> ]	17	17	18	18

\*geotechnical parameters such as Working Platform according in Model 2

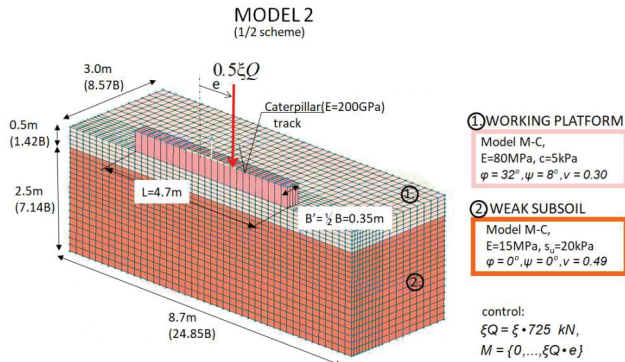


Fig. 3. Example of FE Model - Model 2 (according with Table 1)

Boundary conditions allow for vertical displacement while its normal components are blocked. As the longitudinal axis of a single track is the symmetry axis of the analyzed sub-system, a half-pattern is used ( $B'=0.5B$ ). This significantly shortens the calculation time and does not affect the result of analysis.

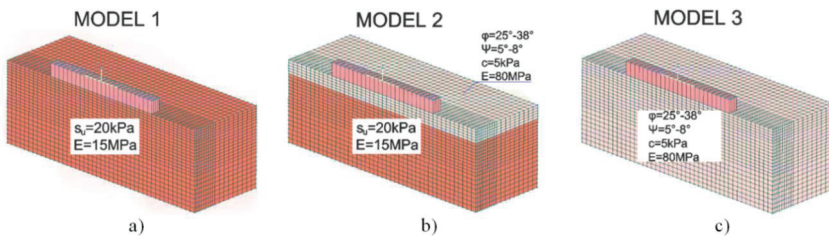


Fig. 4. FE Models: a) Model 1; b) Model 2; c) Model 3

The essential results of the analysis of models: rotation angle –  $\Phi$  and vertical displacement-  $W$  are shown in Fig. 5 – Fig. 10. Functions approximating these characteristics are consistent with the formulas proposed in the article [10].

$$(3.1) \quad \Phi(\xi Q, e_i) = \frac{e_i}{k(\xi)} \cdot \frac{1}{1 - \left(\frac{e_i}{\bar{e}(\xi)}\right)^{a(\xi)}}$$

where:  $k(\xi) = A_k \xi^2 + B_k \xi + C_k$ ;  $\bar{e}(\xi) = A_e \xi^2 + B_e \xi + C_e$ ;  $a(\xi) = A_a \xi^2 + B_a \xi + C_a$

$$(3.2) \quad W(\xi Q, e_i) = \bar{w}(\xi) \frac{1 - S(\xi) e_i^{T(\xi)}}{\left(1 - \frac{e_i}{\bar{e}(\xi)}\right)^{U(\xi)}}$$

where:  $\bar{w}(\xi) = \mu \xi$ ;  $S(\xi) = A_S \xi^2 + B_S \xi + C_S$ ;  $T(\xi) = A_T \xi^2 + B_T \xi + C_T$ ;  $U(\xi) = A_U \xi^2 + B_U \xi + C_U$

Table 2. Coefficients used in approximate formulas for  $k(\xi)$ ,  $\bar{e}(\xi)$ ,  $a(\xi)$

	$A_k$	$B_k$	$C_k$	$A_e$	$B_e$	$C_e$	$A_a$	$B_a$	$C_a$
Model 1	2895	-3656	1144	1.762	-2.78	1.07	82.288	-45.645	14.765
Model 2	1711	-2533	1008	0.047	-1.55	1.212	-26.323	31.888	-4.029
Model 3	3486	-5201	2343	-0.098	-0.37	1.003	-4.640	6.799	0.478

Table 3. Coefficients used in approximate formulas for  $S(\xi)$ ,  $T(\xi)$ ,  $U(\xi)$ ,  $\bar{w}(\xi)$

	$A_S$	$B_S$	$C_S$	$A_T$	$B_T$	$C_T$	$A_U$	$B_U$	$C_U$	$\mu$ [m]
Model 1	868.61	-662.99	126.29	174.35	-140.94	28.29	73.37	-58.56	11.83	-0.00892
Model 2	-23.75	11.14	2.38	0.96	-8.00	6.21	3.95	-4.28	1.41	0.01
Model 3	2.64	-4.12	3.26	2.27	-4.91	3.48	1.77	-1.35	1.26	0.00296

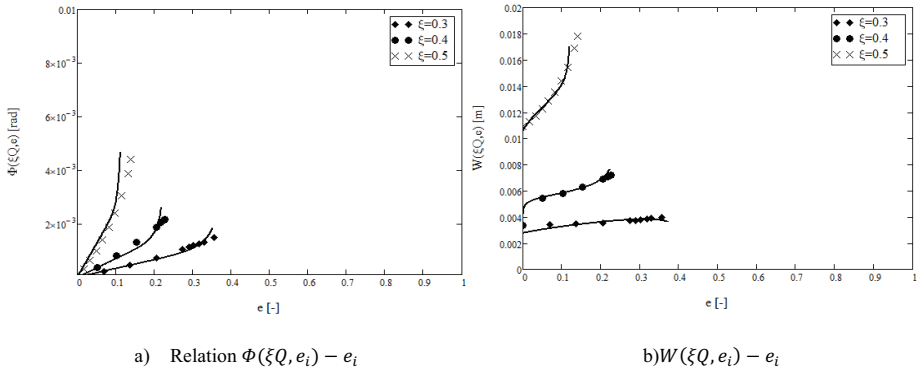


Fig. 5. FE model vs. analytical deformation characteristics for the caterpillar track-subsoil system (Model 1)

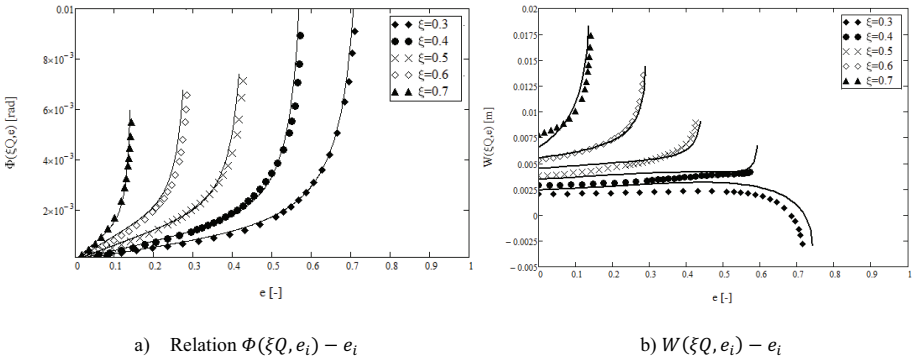
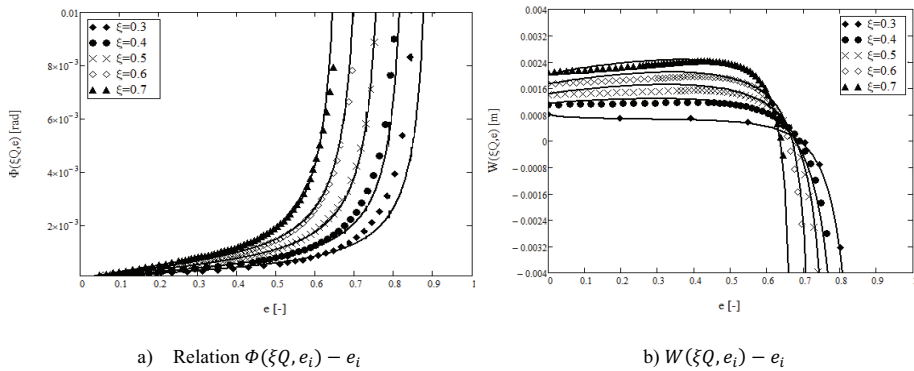


Fig. 6. FE model vs. analytical deformation characteristics for the caterpillar track-subsoil system (Model 2)



a) Relation  $\Phi(\xi Q, e_i) - e_i$  b)  $W(\xi Q, e_i) - e_i$   
 Fig. 7. FE model vs. analytical deformation characteristics for the caterpillar track-subsoil system (Model 3)

## 4. CASE STUDIES

In this paper, a Bauer BG 20H/BT60 drilling rig is considered working on various types of subsoil. All data (geometry, total weight  $Q$ ) are given in Fig. 3. More detailed description can be found in the article [10]. In each analyzed case solution of equations system (2.4)-(2.7) with use of approximate formulas (3.1) and (3.2) are performed with use of MathCad.

### 4.1. CASE STUDY 1

#### ENTRY OF THE MACHINE ON THE GROUND WITH VARIOUS GEOTECHNICAL PARAMETERS UNDER EACH CATERPILLAR TRACKS

In this case study, we assume that the piling rig enters a subgrade with different ultimate bearing capacity and stiffness for each track. Such a case may take place on the construction site if the piling rig goes beyond the designated working platform. The basic set of equations in this case takes the form:

$$(4.1.1) \quad \Phi_{X,1}(\zeta, e_1) = \Phi_{X,2}(1 - \zeta, e_2)$$

$$(4.1.2) \quad \zeta \cdot e_1 + (1 - \zeta) \cdot e_2 = E_X + H_{XX} \cdot \Phi_{X,1}(\zeta, e_1)$$

$$(4.1.3) \quad 2\zeta - 1 = H_{YY} \left( \frac{W_1(\zeta, e_1) - W_2(1 - \zeta, e_2)}{D} \right)$$



$\Phi_{X,1}(\xi, e_1)$  – rotation of one caterpillar track – Model 1 [rad]

$\Phi_{X,2}(1-\xi, e_2)$  – rotation of one caterpillar track – Model 2 [rad]

$W_1(\xi, e_1)$  – vertical displacements under one caterpillar track – Model 1 [m]

$W_2(1-\xi, e_2)$  – vertical displacements under one caterpillar track – Model 2 [m]

$E_X, H_{XX}, H_{YY}$  – kinematic and geometrical parameters of the machine [-], fully described in the article [10]. In the considered case they are:  $E_X = \frac{2}{L} \cdot \bar{x}$ ,  $H_{XX} = \frac{2}{L} \cdot \bar{z}$ ,  $H_{YY} = \frac{2}{D} \cdot \bar{z}$  where  $\bar{x}, \bar{y}, \bar{z}$  are coordinates of gravity center. Scheme of this case is shown in Fig. 8 – Fig. 10.

#### 4.1.1. ENTRY OF CATERPILLAR TRACKS ON THE GROUND WITH VARIOUS GEOTECHNICAL PARAMETERS. MODEL 1 VS MODEL 2.

Scheme of case is shown in Fig. 8.

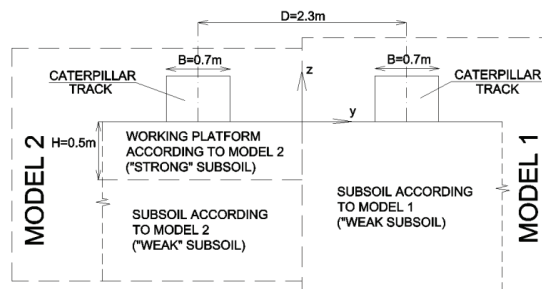


Fig. 8. Scheme of Case Study 1. Interaction of Model 1 and Model 2

Due to the fact that the ultimate bearing capacity of the subsoil according to Model 1 is low, there is a rapid destruction of the subsoil under the caterpillar tracks. The FE analysis and approximate formulas does not allow to determine the value  $\xi$ ,  $e_1$  and  $e_2$ .

**4.1.2. ENTRY OF CATERPILLAR TRACKS ON THE GROUND WITH VARIOUS GEOTECHNICAL PARAMETERS. MODEL 2 VS MODEL 3.**

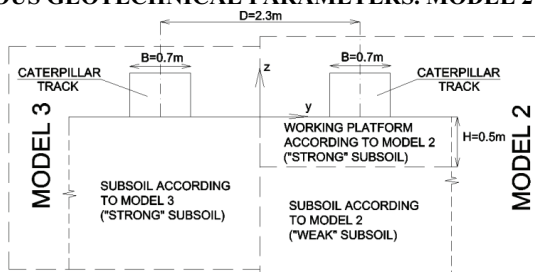


Fig. 9. Scheme of Case Study 1. Interaction of Model 2 and Model 3

For this case second order analysis was performed i.e. additional moments  $M_X^{sec}$ ,  $M_Y^{sec}$  caused by rotations  $\Phi_X$ ,  $\Phi_Y$  (i.e.  $M_X^{sec} = \Phi_X \cdot \bar{z}$ ,  $M_Y^{sec} = \Phi_Y \cdot \bar{z}$ ) are taken into account.

Results of this case study are presented in Table 4.

Table 4. Results of second-order analysis (Model 2 vs Model 3):

	Second-order analysis $E_X=0.345 ; H_{YX}=1.809 ; H_{YI}=3.696$
$\xi$ [-]	0.501
$e_1$ [-]	0.407
$e_2$ [-]	0.286

Second-order analysis:  $\xi = 0.501[-]$  indicates almost symmetrical distribution of loads under the caterpillar track located on Model 2 and a caterpillar track located on Model 3. Such a case ( $\xi \approx 0.5$ -case symmetrical) is the result of a small difference in displacement between caterpillar tracks working on two different subsoil (Model 2 and Model 3).

**4.1.3 ENTRY OF CATERPILLAR TRACKS ON THE GROUND WITH VARIOUS GEOTECHNICAL PARAMETERS AND DIFFERENCE OF LEVELS BETWEEN THEM.**

**MODEL 2 VS MODEL 3 (SAME AS 4.1.2).**

In this case, the maximum difference of levels between two caterpillar tracks is estimated. Modified basic set of equation:

$$(4.1.3.1) \quad \Phi_{X,1}(\zeta, e_1) = \Phi_{X,2}(1 - \zeta, e_2)$$

$$(4.1.3.2) \quad \zeta \cdot e_1 + (1 - \zeta) \cdot e_2 = E_X + H_{XX} \cdot \Phi_{X,1}(\zeta, e_1)$$

$$(4.1.3.3) \quad 2\zeta - 1 = H_{YY}(\psi_{0,Y} + \frac{W_1(\zeta, e_1) - W_2(1 - \zeta, e_2)}{D})$$

where:  $\psi_{0,Y} = \frac{R_z}{D}$

$R_z = W_1 - W_2$  is a difference of levels between the caterpillar tracks. A scheme of the case is shown in Fig. 10.

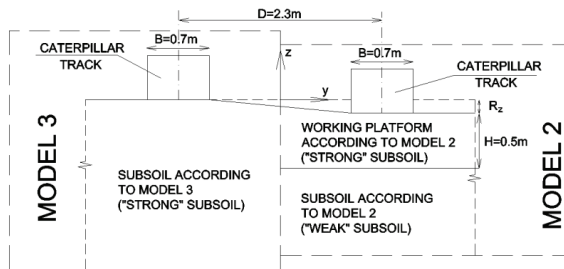


Fig. 10. Scheme of Case Study 1. Interaction of Model 2 and Model 3 (with difference of levels between two caterpillar tracks)

Results are:  $\xi = 0.68 [-]$ ,  $e_1 = 0.79 [-]$ ,  $e_2 = 0.14 [-]$ ,  $R_z = 0.21[m]$ .

At the entry piling rig on the ground with different ultimate bearing capacity and difference of levels between the base of caterpillar tracks, one caterpillar track on Model 2 will take over 68% of the total load ( $\xi = 0.68 [-]$ ) and the maximum dimensionless eccentric  $e_1 = 0.79 [-]$  for the caterpillar track located on Model 2 and  $e_2 = 0.14 [-]$  for the caterpillar track located on Model 3. Maximum levels difference between two caterpillar tracks is  $R_z = 0.21m$  when both are working on subgrades of different bearing capacity. Results of analysis  $\xi(R_z)$ ,  $e_1(R_z)$  and  $e_2(R_z)$  are shown in Fig. 11.

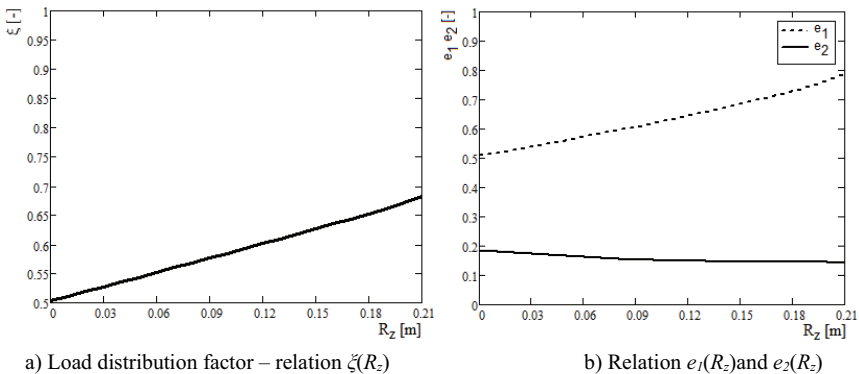


Fig. 11. Results of analysis

Fig. 11a shows how the change in difference of levels between two caterpillar tracks ( $R_z$ ) affects the dimensionless factor ( $\zeta$ ) describing distribution of total machine weight  $Q$  between two caterpillar tracks.

Fig. 11b shows how dimensionless eccentricities of forces acting on one caterpillar track  $e_1$  and  $e_2$  change when the  $R_z$  value changes.

#### 4.1.4 ENTRY OF CATERPILLAR TRACKS ON THE GROUND WITH VARIOUS GEOTECHNICAL PARAMETERS. MODEL 1 VS MODEL 3.

As in chapter 4.1.1, it is impossible to determine the values of the parameters  $\zeta$ ,  $e_1$  and  $e_2$ .

### 4.2. CASE STUDY 2 DEFINITION OF THE MAXIMUM PERMISSIBLE ANGLE OF GROUND SLOPE

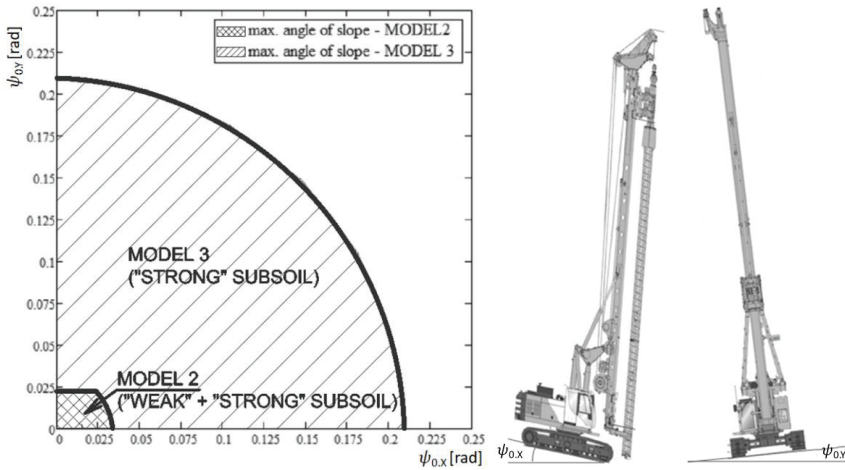
Loss of stability means that the machine will overturn. We distinguish the concept of longitudinal stability (overturn of the machine along its basic direction of moving) or lateral stability (overturn of the machine perpendicular to basic direction of moving). In this case, the maximum permissible angle of ground slope for the machine sliding off the slope is determined (a more unfavorable situation due to the center of gravity of the machine). Basic set of equations:

$$(4.2.1) \quad \Phi_{X,1}(\zeta, e_1) = \Phi_{X,2}(1 - \zeta, e_2)$$

$$(4.2.2) \quad \zeta \cdot e_1 + (1 - \zeta) \cdot e_2 = E_X + H_{XX}(\psi_{0,X} + \Phi_{X,1}(\zeta, e_1))$$

$$(4.2.3) \quad 2\zeta - 1 = H_{YY}(\psi_{0,Y} + \frac{W(\zeta, e_1) - W(1 - \zeta, e_2)}{D})$$

where:  $\psi_{0,X}, \psi_{0,Y}$  – angle of slope in the  $X, Y$  direction [rad] which was incrementally increased, which assumed ratio between angles  $\psi_{0,X}, \psi_{0,Y}$ , up to divergent state when solution was impossible to obtain.



a) Model 2 and Model 3                      b) Marking the angle of slope  
 Fig. 12. Maximum permissible angle of slope

## 5. FINAL CONCLUSIONS

The main purpose of this article is to show the possibilities of creating algorithms for designing a working platform. Two exemplary problems are presented in this article - the entry of the machine on the ground with various geotechnical parameters under each caterpillar tracks and detection of the maximum permissible angle of ground slope. The solution of these two problems is based on the development of the basic assumptions contained in the previous publication on the issue of stability of drilling rigs [10]. These problems show real work of piling rigs on the construction site, if the machine goes out of the working platform or piling rig goes down the slope. This publication only covers two cases that should be considered when designing working

platforms. Analysis of other practically important cases was presented in [9], more of this and complete algorithm of design will be done in future publications.

## REFERENCES

1. K. Białek, L. Bałachowski, "Bearing capacity of the working platform with kinematic method", *StudiaGeotech Mech*,37(1), 2015.
2. H.J. Burd, S. Frydman, "Bearing capacity of plane-strain footings on layered soils", *Canadian Geotechnical Journal*;34,p.241–53, 1997.
3. W.F. Chen H.L. Davidson, "Bearing capacity determination by limit analysis", Fritz Engineering Laboratory Report , 355(15) ,1972.
4. D.V. Griffiths, "Computation of bearing capacity on layered soil", *Proceedings of the4th international conference on numerical methods in geomechanics*, vol. 1, p. 163–70, 1982.
5. A.M. Hanna, G.G. Meyerhof, "Design charts for ultimate bearing capacity of foundations on sand overlying soft clay", *Canadian Geotechnical Journal*, 17, p.300–309, 1980.
6. R.L. Michałowski, L. Shi, "Bearing capacity of footings over two-layer foundation soils", *Journal of Geotechnical Engineering*,121(5), p.421–428, 1995.
7. P.W. Mitchell, "Bearing capacity of shallow footings in sand over clay by the punching shear model", *Australian Geomechanics*,41(2), 2006.
8. Piling & Foundation Specialists Federation. Web page<http://www.pilingfederation.org.au/page/pilesafe.html>
9. Richter M., Urbański A., "Stability of drilling rigs" (in Polish *Stateczność maszyn budowlanych*), *Builder*, Vol. 8 (253), 2018.
10. A. Urbański, A. Truty, M. Richter, "Stability of drilling rigs moving on a weak subsoil. Theoretical formulation and selected case studies", *Engineering Structures*, Vol. 184, 2019.
11. Working platforms for tracked plant: good practice guide to the design, installation, maintenance and repair of ground-supported working platforms, BRE 470, Garston, Watford: BRE Press, 2004.
12. ZSOIL.PC 2016. User manual, 2016.

## LIST OF FIGURES AND TABLES:

Fig. 1. Basic components of statical and kinematical models

Rys. 1. Podstawowe elementy modeli statycznych i kinematycznych

Tab. 1. Material properties of soils

Tab. 1. Parametry materiałowe podłoża gruntowego

Fig. 2 Characteristics rotation - eccentricity of subsoil-rigid body system (caterpillar tracks) in unilateral contact problem for the case of subsoil type : a) rigid; b) elastic; c) rigid-plastic; d) elastic-plastic

Rys. 2. Charakterystyki obrót-mimośrodek systemu podłoże-bryła sztywna (układ gąsienicowy) w zadaniu kontaktowym dla przypadku podłoża: a) sztywnego; b) sprężystego; c) sztywno-plastycznego; d) sprężysto-plastycznego

Tab. 2. Coefficients used in approximate formulas for  $k(\zeta)$ ,  $\bar{e}(\zeta)$ ,  $a(\zeta)$

Tab. 2. Współczynniki używane w formułach aproksymujących  $k(\zeta)$ ,  $\bar{e}(\zeta)$ ,  $a(\zeta)$

Fig. 3. Example of FE Model - Model 2 (according with Table 1)

Rys. 3. Przykład MES – Model 2 (zgodnie z Tabela 1)

Tab. 3. Coefficients used in approximate formulas for  $S(\zeta)$ ,  $T(\zeta)$ ,  $U(\zeta)$ ,  $\bar{w}(\xi)$

Tab. 3. Współczynniki używane w formułach aproksymujących  $S(\zeta)$ ,  $T(\zeta)$ ,  $U(\zeta)$ ,  $\bar{w}(\xi)$

Fig. 4. FE Models: a) Model 1; b) Model 2; c) Model 3

Rys. 4. Modele MES: a) Model 1; b) Model 2; c) Model 3

Tab. 4. Results of second-order analysis (Model 2 vs Model 3)

Tab. 4. Wyniki analizy drugiego rzędu (Model 2 vs Model 3)

Fig. 5. FE model vs. analytical deformation characteristics for the caterpillar track-subsoil system (Model 1)

Rys. 5. Model MES vs. analityczne charakterystyki deformacji gąsienicowy układ bieżny - podłoże gruntowe (Model 1)

Fig. 6. FE model vs. analytical deformation characteristics for the caterpillar track-subsoil system (Model 2)

Rys. 6. Model MES vs. analityczne charakterystyki deformacji gąsienicowy układ bieżny – podłoże gruntowe (Model 2)

Fig. 7. FE model vs. analytical deformation characteristics for the caterpillar track-subsoil system (Model 3)

Rys. 7. Model MES vs. analityczne charakterystyki deformacji gąsienicowy układ bieżny - podłoże gruntowe (Model 3)

Fig. 8. Scheme of Case Study 1. Interaction of Model 1 and Model 2

Rys. 8. Schemat Stadium Przypadku nr 1. Zależności pomiędzy Modelem 1 i Modelem 2

Fig. 9. Scheme of Case Study 1. Interaction of Model 2 and Model 3

Rys. 9. Schemat Stadium Przypadku nr 1. Zależności pomiędzy Modelem 2 i Modelem 3

Fig. 10. Scheme of Case Study 1. Interaction of Model 2 and Model 3 (with difference of levels between two caterpillar tracks)

Rys. 10. Schemat Stadium Przypadku nr 1. Zależności pomiędzy Modelem 2 i Modelem 3 (z różnicą wysokości pomiędzy gąsienicami)

Fig. 11. Results of analysis: a) Load distribution factor – relation  $\zeta(R_z)$ ; b) Relation  $e_1(R_z)$  and  $e_2(R_z)$

Rys. 11. Rezultaty analizy: a) Współczynnik rozdziału obciążeń – zależność  $\zeta(R_z)$ ; b) Zależność  $e_1(R_z)$  i  $e_2(R_z)$

Fig. 12. Maximum permissible angle of slope for: a) Model 2 and Model 3; b) Marking the angle of slope

Rys. 12. Maksymalny dopuszczalny kąt nachylenia terenu: a) dla Modelu 2 i Modelu 3; b) Oznaczenie kątów nachylenia terenu

## ANALIZA STATECZNOŚCI WIERTNIC PORUSZAJĄCYCH SIĘ PO PODŁOŻU SŁABONOŚNYM. STUDIUM WYBRANYCH PRZYPADKÓW

*Słowa kluczowe:* platformy robocze, interakcja podłoże gruntowe - maszyna, palownica, nośność podłoża, inżynieria geotechniczna, modelowanie metodą elementów skończonych

### PODSUMOWANIE:

Nabierająca tempa dynamika produkcji budowlanej wymusza na inwestorach konieczność zagospodarowania nieruchomości gruntowych których przeznaczenie na cele budowlane było wcześniej nieopłacalne (niskie parametry gruntowe, wysoki poziom wód gruntowych, występowanie zwartej zabudowy itp.). W związku z tym, grunty na których posadowienie są budynki coraz częściej charakteryzują się niskimi parametrami wytrzymałościowymi. Dlatego

geotechnicy mają trudne zadanie projektowania i wykonywania budowli na terenach wymagających podjęcia szczególnych środków ostrożności. W celu odpowiedniego przenoszenia obciążeń pomiędzy budynkiem a podłożem gruntowym o niskich parametrach wytrzymałościowych projektanci decydują się na wykonanie fundamentów pośrednich. Ich wykonanie wymaga zastosowania specjalistycznych maszyn roboczych (palownic, wiertnic itp.). Przed dopuszczeniem maszyny roboczej do pracy należy sprawdzić, czy podłoże gruntowe ma wystarczającą nośność. W przypadku jej niedoboru, należy odpowiednio wzmocnić podłoże poprzez wykonanie platformy roboczej. W niniejszym artykule przedstawiono analizę współpracy maszyna budowlana - podłoże gruntowe. Podstawową analizę przeprowadzono metodą elementów skończonych 3D (oprogramowanie FE ZSoil.PC). Jej wyniki zostały opracowane w formie formuł umożliwiających rozwiązanie problemu interakcji maszyna budowlana – podłoże gruntowe. Szczegółowe obliczenia przeprowadzono dla palownicy - Bauer BH20H (BT60). Publikacja została podzielona na pięć głównych części:

#### 1. Wprowadzenie

Omówiono dotychczasowe publikacje dotyczące określenia nośności podłoża gruntowego składającego się z warstw o różnych wartościach parametrów geotechnicznych. Wcześniejsze badania obejmują głównie rozwiązania w płaskim stanie odkształcenia.

#### 2. Założenia

- I. Maszyna przekazuje obciążenia na podłoże gruntowe za pomocą gąsienicowego układu bieżnego,
- II. Cała maszyna (w tym dwie gąsienice) traktowana jest jako bryła sztywna,
- III. Zamodelowano podłoże podatne, model sprężysto-plastyczny Coulomba – Mohra (implementacja w programie Zsoil.PC),
- IV. Pominięto nakładanie się stref oddziaływań poszczególnych gąsienic na podłoże gruntowe.

#### 3. Analiza. Analizę przeprowadzono dla trzech modeli obliczeniowych:

MODEL 1: składające się z warstwy spoistego podłoża gruntowego o parametrach:  $s_u=20\text{kPa}$ ,  $E=15\text{MPa}$  (słabe podłoże gruntowe),

MODEL 2: składające się z warstwy spoistego podłoża gruntowego o parametrach:  $s_u=20\text{kPa}$ ,  $E=15\text{MPa}$  (słabe podłoże gruntowe) oraz ułożonej na jej górnej warstwie platformy roboczej o grubości  $H=0,5\text{m}$  o parametrach  $\phi=32^\circ$  ( $\psi=8^\circ$ ),  $c=5\text{kPa}$ ,  $E=80\text{MPa}$ ,

MODEL 3: warstwa z której zbudowana jest platforma robocza:  $\phi=32^\circ$  ( $\psi=8^\circ$ ),  $c=5\text{kPa}$ ,  $E=80\text{MPa}$ .

#### 4. Studium przypadku

Wykonano studium przypadku dla dwóch często spotykanych na placu budowy przypadków:

I) wjazdu maszyny na podłoże o różnej nośności pod gąsienicami (1 – przy braku różnicy wysokości pomiędzy gąsienicami, 2 – przy różnicy wysokości pomiędzy gąsienicami),

II) określenia maksymalnego dopuszczalnego pochylenia terenu umożliwiającego bezpieczne poruszanie się maszyny przy zjeździe ze skarpy.



Rozwiązaniem I studium przypadku jest określenie granicznych wartości  $\xi$ ,  $e_1$ ,  $e_2$  które są podstawowymi wartościami służącymi do projektowania platform roboczych. Rozwiązaniem II studium przypadku jest określenie maksymalnych dopuszczalnych kątów nachylenia terenu ( $\psi_{0,X}$ ,  $\psi_{0,Y}$ ) przy zjeździe palownicy ze skarpy.

#### 5. Podsumowanie

Głównym celem tego artykułu jest pokazanie możliwości stworzenia algorytmu pozwalającego na projektowanie platform roboczych. W tym artykule przedstawiono dwa problemy, które zostały omówione w rozdziale 4. Rozwiązanie tych dwóch problemów opiera się na opracowaniu podstawowych założeń zawartych w poprzedniej publikacji autorów na temat stabilności ciężkich gąsienicowych maszyn budowlanych (palownic, wiertnic). Niniejsza publikacja obejmuje tylko przykładowe dwa przypadki, na które należy zwrócić uwagę przy projektowaniu platform roboczych.

Received 5.11.2019, Revised 21.04.2020

